Drebrin A regulates dendritic spine plasticity and synaptic function in mature cultured hippocampal neurons

Anton Ivanov[1], Monique Esclapez[2], Christophe Pellegrino[1], Tomoaki Shirao[3] and Lotfi Ferhat[1,4,*]

[1]INMED/INSERM U29, Parc Scientifique de Luminy, 13273, Marseille, France
[2]INSERM U 751, Université d'Aix-Marseille, Hôpital de la Timone, Marseille, France
[3]Department of Neurobiology and Behavior, Gunma University Graduate School of Medicine, Maebashi, Gunma, Japan
[4]CNRS UMR 6184, Neurobiologie des Interactions Cellulaires et Neurophysiopathologie (NICN), IFR Jean Roche, Marseille, F-13020, France
*Author for correspondence (e-mail: lotfi.ferhat@univmed.fr)

Accepted 30 October 2008
Journal of Cell Science 122, 524-534 Published by The Company of Biologists 2009
doi:10.1242/jcs.033464

Summary

Drebrin A, one of the most abundant neuron-specific F-actin-binding proteins, is found exclusively in dendrites and is particularly concentrated in dendritic spines receiving excitatory inputs. We investigated the role of drebrin A in synaptic transmission and found that overexpression of drebrin A augmented the glutamatergic synaptic transmission, probably through an increase of active synaptic site density. Interestingly, overexpression of drebrin A also affected the frequency, amplitude and kinetics of miniature inhibitory postsynaptic currents (mIPSCs), despite the fact that GABAergic synapse density and transmission efficacy were not modified. Downregulation of drebrin A led to a decrease of both glutamatergic and GABAergic synaptic activity. In heterologous cells, drebrin A reorganized and stabilized F-actin and these effects were mediated by its actin-binding domain. Thus, drebrin A might regulate dendritic spine morphology via regulation of actin cytoskeleton remodeling and dynamics. Our data demonstrate for the first time that drebrin A modulates glutamatergic and GABAergic synaptic activities.

Supplementary material available online at
http://jcs.biologists.org/cgi/content/full/122/4/524/DC1

Key words: Spine morphogenesis, F-actin, GABA, Glutamate, vGlut1, Gad-65, Bassoon

Introduction

Dendritic spines are the postsynaptic elements that receive the majority of excitatory glutamatergic inputs in the CNS (Harris and Kater, 1994). These small protrusions emerging from dendritic shafts are believed to constitute sites for the development of glutamatergic neuronal networks and might be a cellular substrate for synaptic plasticity (Yuste and Bonhoeffer, 2001).

The actin filament (F-actin) is one of the major structural elements of dendritic spines (Fifkova and Delay, 1982; Matus et al., 1982). These actin filaments are thought to be the key target of molecular mechanisms regulating spine plasticity that has been shown to be activity dependent (Matus, 2000). The adult isoform of drebrin, drebrin A (DA), a major neuron-specific F-actin-binding protein, emerges as a candidate protein that regulates the actin cytoskeleton of dendritic spines (Sekino et al., 2007). DA is specifically localized at dendritic spines of mature cortical neurons (Hayashi et al., 1996; Aoki et al., 2005) and is known to inhibit the actin-binding activity of tropomyosin, fascin and α-actinin (Ishikawa et al., 1994; Sasaki et al., 1996). In vitro, it also inhibits the interaction between actin and myosin (Hayashi et al., 1996; Ishikawa et al., 2007), suggesting that it modulates actin filament contractility. Transfection of DA into fibroblasts induced reorganization of actin filaments, leading to a change in cell morphology (Shirao et al., 1994). Such transfection in neurons results in the elongation of dendritic spines of cortical neurons (Hayashi and Shirao, 1999). Furthermore, downregulation of DA expression in developing hippocampal neurons suppresses the accumulation of F-actin within dendritic spines (Takahashi et al., 2003).

In addition to its role in spine morphology, DA might be involved in spine functions. It has been recently shown that DA is involved in spinous clustering of the postsynaptic density (PSD) scaffold protein, PSD-95 (Takahashi et al., 2003), as well as in the activity-dependent synaptic targeting of N-methyl-D-aspartate (NMDA) subtype of glutamate receptors (Takahashi et al., 2006). Consistent with this observation, the induction of long-term potentiation (LTP) in the hippocampus is accompanied by the enhanced DA content within dendritic spines (Fukazawa et al., 2003). All these data support the hypothesis that DA expressed in spines can modulate synaptic activity.

To test this hypothesis, we investigated the effects of DA on dendritic spine morphology and its consequences on synaptic activity, in mature cultured hippocampal neurons. Our study led to three main conclusions: (1) the actin-binding domain of DA is responsible for dendritic spine plasticity, presumably via regulation of actin cytoskeleton remodeling and dynamics; (2) enhanced expression of DA increases the density of glutamatergic but not GABAergic synapses and leads to alteration of the normal excitatory-inhibitory balance in favour of excitation; (3) downregulation of DA results in the decrease of both glutamatergic and GABAergic synaptic transmissions without affecting the normal excitatory-inhibitory balance. Thus, the present study provides the first evidence that an actin-binding protein such as DA modulates both glutamatergic and GABAergic synaptic transmission in mature hippocampal neurons.

Results

Postsynaptic localization of endogenous DA in mixed hippocampal cultures

The developmental changes of DA localization in hippocampal neurons have been described in low-density culture from 7 to 21 days in vitro (DIV) (Takahashi et al., 2003). In this study, we re-examined this issue in mixed high-density hippocampal cultures (supplementary material Fig. S1A,B). Our data confirmed the postsynaptic localization of DA in mixed hippocampal neurons at 21 DIV, because it colocalized with two specific markers for the postsynaptic compartment, PSD-95 and F-actin, in most spines (supplementary material Fig. S1C-E).

The actin-binding domain of DA is responsible for spine morphological changes induced by overexpression of DA-GFP in mature hippocampal neurons

It has been shown that DA affects some morphological aspects of cortical dendritic spines (Hayashi and Shirao, 1999). To analyze the physiological consequences of morphological changes induced by DA, we re-examined the effects of DA on spine morphology in our mature and high-density hippocampal culture system. As revealed by cotransfected red fluorescent protein (RFP) neurons (Fig. 1A,B), both green fluorescent protein (GFP, used as a control) (Fig. 1A′) and DA-GFP (Fig. 1B′) were distributed within dendritic shafts, as well as in dendritic protrusions. With respect to DA-GFP, the green fluorescence in dendritic shafts was lighter than in dendritic protrusions. Striking morphological changes were observed between dendritic protrusions of DA-GFP- (Fig. 1B′) and those of GFP neurons (Fig. 1A′). Indeed, the dendrites of DA-GFP neurons displayed longer protrusions (Fig. 1B-B″, arrows) compared with those found in GFP neurons (Fig. 1A-A″). Some of these long protrusions reached over 5 µm (see asterisks in Fig. 1B-B″). All protrusions induced by DA-GFP included heads, and thus differed in their morphology from dendritic filopodia, which have no heads. These observations suggested that these long protrusions were spines and were more mature than filopodia, which are precursors of dendritic spines (Papa et al., 1995).

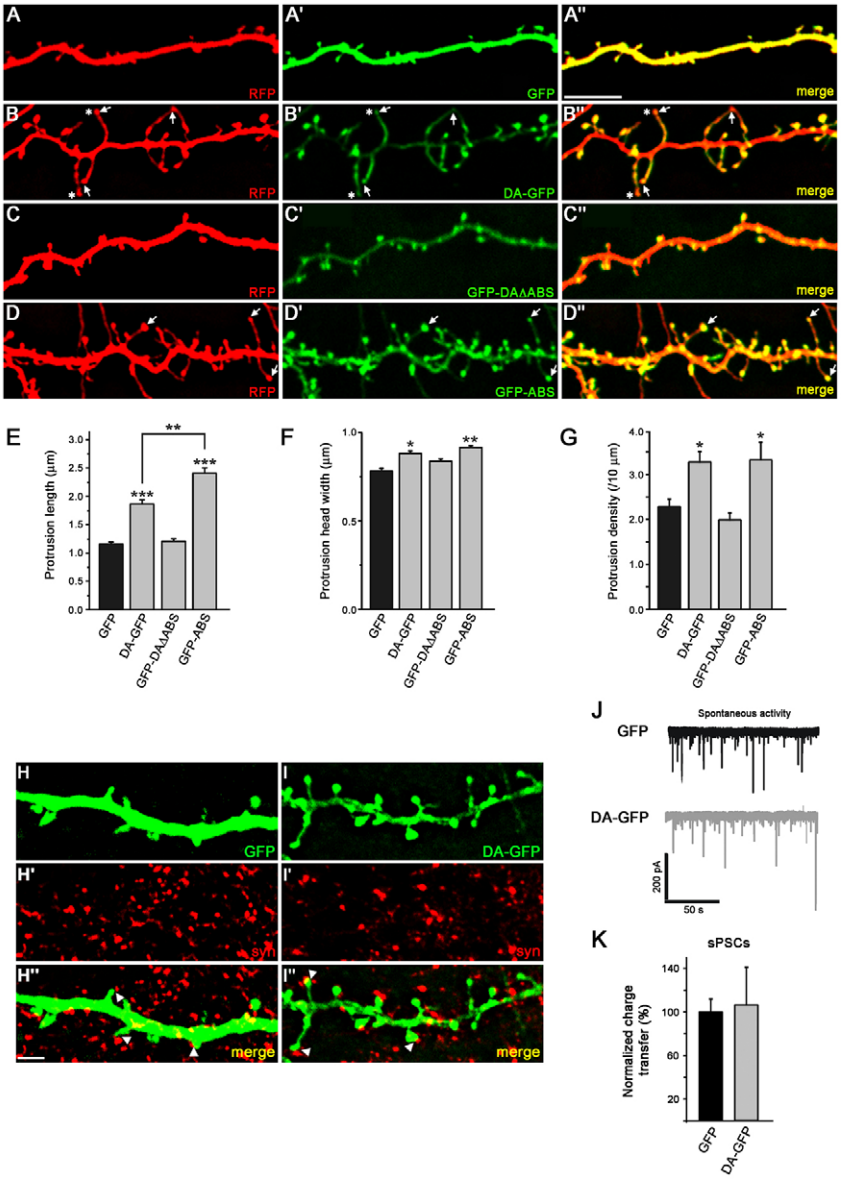

Fig. 1. Effects of DA-GFP overexpression on spine morphology and network activity. Cultured neurons were cotransfected on DIV 21 with RFP (A) and GFP (A′), RFP (B) and DA-GFP (B′), RFP (C) and GFP-DAΔABS (C′), or RFP (D) and GFP-ABS (D′). At 23 DIV, neurons were fixed and then analyzed. RFP channel is shown in all panels to outline dendritic morphology. (A″,B″,C″ and D″) Merged images. Scale bar: 10 µm. (E-G) Quantification of DA-GFP effects on protrusion plasticity. Histograms showing the average length (E), width (F) and density (G) of protrusions of GFP, DA-GFP, GFP-DAΔABS and GFP-ABS neurons. As with GFP spines (H-H″), the long spines induced by DA-GFP (I-I″) were associated with functional excitatory synaptic contacts. GFP (H) or DA-GFP (I) neurons immunostained for synaptophysin (H′ and I′). (H″ and I″) Merged images. Some synaptophysin clusters are not in close apposition to the spines of GFP or DA-GFP neurons because they are probably opposed to dendritic shafts or spines of nontransfected neurons. Scale bar: 10 µm. *P<0.05, **P<0.01, ***P<0.001, Bonferroni's test. (J) Examples of sPSCs recorded at –60 mV in GFP (black trace) and DA-GFP neurons (gray trace). (K) Histogram showing the sPSCs charge transfer in all recorded GFP and DA-GFP neurons. All data in E-G and K are mean ± s.e.m.

To investigate whether DA-GFP exerts its effects via its interaction with F-actin, we cotransfected mature hippocampal neurons with RFP (Fig. 1C) and GFP-DAΔABS (Fig. 1C′), a mutant of DA that lacks the actin-binding domain (Hayashi et al., 1999). As revealed by coexpressed RFP (Fig. 1C), GFP-DAΔABS (Fig. 1C′) was detected in dendritic shafts as well as at dendritic protrusions (Fig. 1C″). In contrast to DA-GFP, GFP-DAΔABS did not induce elongation of dendritic protrusions (Fig. 1C-C″). These data indicate that the elongation of dendritic protrusions induced by DA-GFP requires its actin-binding domain.

We further determined whether the overexpression of the actin-binding domain of DA was sufficient to induce the elongation of dendritic protrusions. For this purpose, we cotransfected hippocampal neurons with RFP (Fig. 1D) and GFP-ABS (Fig. 1D′), a construct that contains only the actin-binding domain of DA (Hayashi et al., 1999). As visualized by cotransfected RFP (Fig. 1D), GFP-ABS was found in dendritic shafts as well as in dendritic protrusions (Fig. 1D″). Similarly to DA-GFP, GFP-ABS induced morphological changes in dendritic protrusions. Indeed, some dendritic protrusions of GFP-ABS neurons were markedly longer (Fig. 1D-D″, see arrows) than those observed in GFP neurons (Fig. 1A-A″). In addition, GFP-ABS neurons displayed long protrusions with heads, reminiscent of dendritic spines. Therefore, the actin-binding domain of DA is necessary and sufficient to induce an effect on dendritic spine elongation.

Quantitative analysis in both DA-GFP and GFP-ABS neurons showed that the average protrusion lengths were significantly longer (1.86±0.08 and 2.40±0.10 μm, respectively) than that in GFP (1.15±0.04 μm; n=10; P<0.001; Bonferroni's test) (Fig. 1E) and GFP-DAΔABS neurons (1.15±0.04 and 1.21±0.04 μm, respectively; n=10; P<0.001; Bonferroni's test) (Fig. 1E). However, the average protrusion length of GFP-DAΔABS neurons was not significantly different from that of GFP neurons (P=0.38; Bonferroni's test) (Fig. 1E). Interestingly, the average protrusion of GFP-ABS was significantly longer than that in DA-GFP neurons (P<0.01; Bonferroni's test) (Fig. 1E), presumably due to their differences in expression levels. Indeed, western blot analyses on CHO-K1 cells showed higher expression levels of GFP-ABS compared with those of DA-GFP construct (data not shown).

In DA-GFP and GFP-ABS neurons, the average protrusion head width was significantly larger (0.88±0.02 and 0.91±0.01 μm, respectively) than that in GFP neurons (0.78±0.02 μm; n=10; P<0.05 for DA-GFP and P<0.01 for GFP-ABS; Bonferroni's test) (Fig. 1F). However, in GFP-DAΔABS neurons, the average protrusion head width (0.83±0.01 μm) was not different from that of GFP neurons (n=10; P=0.18; Bonferroni's test) (Fig. 1F).

In DA-GFP and GFP-ABS neurons, the average protrusion densities were significantly higher (3.28±0.23 and 3.32±0.39 spines/10 μm, respectively) than that in GFP neurons (2.29±0.17 spines/10 μm; n=10; P<0.05; Bonferroni's test) (Fig. 1G), whereas the average protrusion density of GFP-DAΔABS neurons (2.00±0.15 spines/10 μm) was not significantly different from that of GFP neurons (n=10; P=0.26; Bonferroni's test) (Fig. 1G). Therefore the actin-binding domain of DA was necessary and sufficient to induce an effect on spine morphology.

The molecular mechanisms by which DA-GFP causes elongation of dendritic spines was investigated. For this purpose, we overexpressed either DA-GFP or its DA mutants (GFP-DAΔABS and GFP-ABS) in CHO-K1 cells and analyzed its effects on the organization and stabilization of F-actin (supplementary material Figs S2 and S3, respectively). CHO-K1 cells were used because, in contrast to neurons, they provide a model of choice for visualizing the cellular organization and stability of F-actin (Rami et al., 2006). Studies in heterologous cells revealed that DA reorganized F-actin and stabilized them and these effects were dependent upon its actin-binding domain (supplementary material Figs S2 and S3, respectively).

Effects of DA-GFP overexpression on synaptic function

Our confocal microscopy data revealed that as for spines labeled with GFP (Fig. 1H-H″, see arrowheads), the long protrusions induced by DA-GFP (Fig. 1I) were associated with axon terminals since a presynaptic marker such as synaptophysin (Fig. 1I′) was facing most of these dendritic protrusions (Fig. 1I″, arrowheads). The close apposition of the presynaptic marker to the long spines induced by overexpression of DA-GFP suggests the presence of synaptic excitatory contacts. We next investigated whether these synapses were functional. Whole-cell recordings of spontaneous and miniature synaptic currents were performed on mature cultured hippocampal neurons overexpressing either GFP (used as a control, supplementary material Fig. S4) or DA-GFP. Our data showed that spontaneous activity was detected both in GFP or DA-GFP neurons (Fig. 1J), indicating that these neurons were alive and integrated in the neuronal network. In addition, the neuronal network activity was not affected by the overexpression of DA-GFP compared with that of GFP neurons. Indeed, the average charge transfer of spontaneous postsynaptic currents (sPSCs) was not significantly different in both culture types (GFP, 100±11%; DA-GFP, 106±35%; $n \geqslant 5$; P=0.8; U-test) (Fig. 1K).

Next, we investigated whether overexpression of DA-GFP was also associated with changes in the electrophysiological properties of excitatory glutamatergic synapses (Fig. 2A). In DA-GFP neurons, the cumulative probability plots of amplitude (Fig. 2B) and frequency (Fig. 2C) of miniature excitatory postsynaptic currents (mEPSCs) were significantly shifted to higher values compared with those of GFP neurons (n=8; P<0.01 for the amplitude and P<0.05 for the frequency; K-S test). The average amplitude and frequency of mEPSCs were increased in DA-GFP neurons (14.0±0.6 pA; 3.7±0.5 Hz) when compared with those of GFP neurons (11.8±0.4 pA, Fig. 2B, inset; 2.9±0.5 Hz, Fig. 2C, inset). However, the average rise times (GFP: 1.28±0.26 mseconds; DA-GFP: 1.16±0.11 mseconds; n=8; P=0.67; Student's t-test) (Fig. 2D) and decay times (GFP, 6.04±0.90 mseconds; DA-GFP, 6.39±0.79 mseconds; n=8; P=0.14; Student's t-test) (Fig. 2E) were comparable. As a result of the amplitude and frequency changes of mEPSCs in DA-GFP neurons, the average charge transfer of mEPSCs was significantly increased in DA-GFP neurons (334±93 vs 100±20%; n=8; P<0.01; U-test) (Fig. 2F).

The GABA miniature inhibitory postsynaptic currents (mIPSCs) were also recorded from the same GFP and DA-GFP neurons (Fig. 3A) used for mEPSC recordings. Surprisingly, the effects of DA-GFP overexpression on GABA transmission were more severe than those on glutamate transmission. In neurons overexpressing DA-GFP, cumulative probability plots of mIPSC amplitude were significantly shifted to lower values compared with those of GFP neurons (n=8; P<0.01; K-S test) (Fig. 3B). The average amplitude of mIPSCs was lower in DA-GFP neurons (24.0±0.9 pA) than in GFP neurons (34.3±1.8 pA) (Fig. 3B, inset). However, the cumulative probability plots of mIPSC frequency in DA-GFP neurons were significantly shifted to higher values compared with those of GFP neurons (n=8; P<0.001; K-S test) (Fig. 3C). The average frequency of mIPSCs was higher in neurons overexpressing

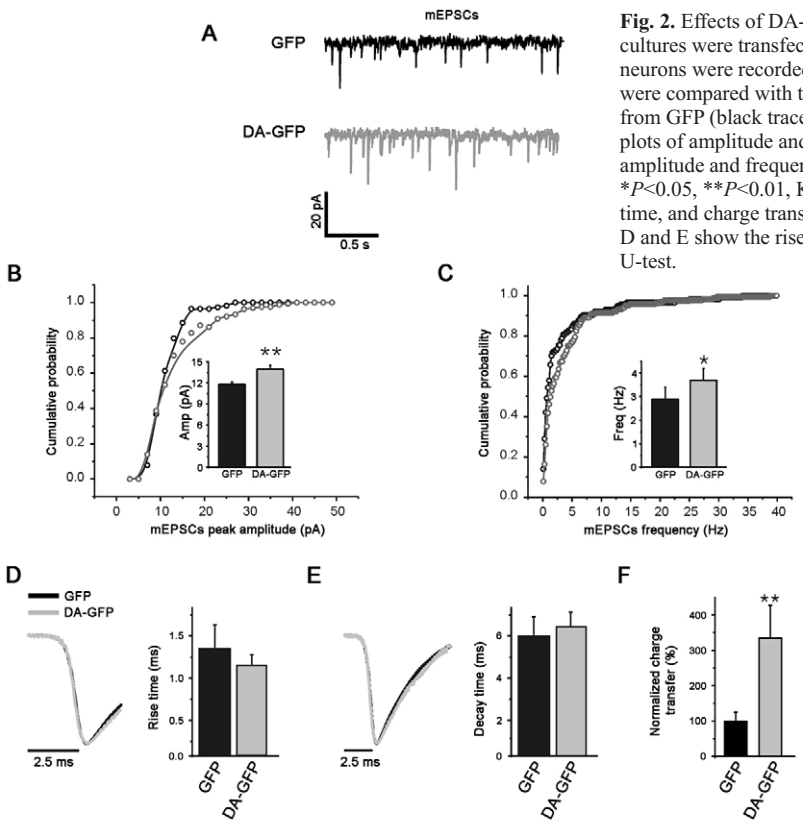

Fig. 2. Effects of DA-GFP overexpression on glutamate function. Mixed hippocampal cultures were transfected at 21 DIV with GFP or DA-GFP, and 1 day later, the transfected neurons were recorded. Electrophysiological recordings of GFP neurons used as controls were compared with those of DA-GFP neurons. (A) Examples of mEPSCs recordings from GFP (black trace) and DA-GFP neurons (gray trace). (B,C) Cumulative probability plots of amplitude and frequency of mEPSCs in GFP and DA-GFP neurons. The average amplitude and frequency of mEPSCs in GFP and DA-GFP neurons are shown as insets. **P*<0.05, ***P*<0.01, K-S test. (D-F) Histograms showing the average rise time, decay time, and charge transfer of mEPSCs respectively in GFP and DA-GFP neurons. Traces in D and E show the rise and decay time, respectively, of the average mEPSCs. ***P*<0.01, U-test.

DA-GFP (2.8±0.3 Hz) than in GFP neurons (1.3±0.2 Hz; *n*=8) (Fig. 3C, inset). The average rise time of mIPSCs was significantly increased in DA-GFP neurons (4.28±0.64 mseconds) when compared with that of GFP neurons (1.84±0.16 mseconds; *n*=8; *P*<0.05; Student's *t*-test) (Fig. 3D), whereas the average decay time was significantly decreased (18.93±1.46 vs 23.38±2.41 mseconds; *n*=8; *P*<0.05; Student's *t*-test) (Fig. 3E). However, despite the mIPSC properties changes described above, the average charge transfer in neurons overexpressing DA-GFP (132±33%) was not significantly different from that of GFP neurons (100±3%; *n*=8; *P*=0.23; U-test) (Fig. 3F).

Thus, the overexpression of DA-GFP displayed differential effects on functional properties of excitatory and inhibitory synapses. Indeed, DA enhances the strength of excitatory synaptic transmission preferentially (Fig. 2F), without affecting the efficacy of inhibitory synaptic transmission (Fig. 3F). As a result, the average inhibition to excitation charge transfer ratio was significantly reduced in DA-GFP neurons (5.5±0.2) when compared with that of GFP neurons (11.2±0.5; *n*=8; *P*<0.01; U-test) (Fig. 3G).

The effects of DA-GFP on synaptic proteins

The changes in GABA and glutamate miniature postsynaptic current (mPSC) properties induced by DA-GFP prompted us to examine whether the density of glutamate and GABA receptors were affected. The quantitative analysis revealed that DA overexpression did not modify significantly the average current density [amplitude (pA)/cell capacitance (pF)] of the agonist-mediated responses compared with that of GFP neurons, which were used as a control (isoguvacine, 8.9±1.8 vs 8.7±2.2, *P*=0.93; AMPA, 3.9±2.1 vs 6.3±3.7, *P*=0.39; NMDA, 2.2±0.6 vs 1.8±0.3; *n*≥9; *P*=0.37; Student's *t*-test) (Fig. 4B). These results suggested that the density of $GABA_A$, AMPA, and NMDA membrane receptors were comparable in both GFP and DA-GFP neurons.

We therefore assessed whether postsynaptic expression of DA-GFP might affect the density of glutamatergic and GABAergic presynaptic terminals (Fig. 4C). These terminals were identified with synaptophysin (the general presynaptic marker) or transmitter-specific markers of glutamatergic and GABAergic axons (vGlut1 and Gad-65, respectively). The average densities of synaptophysin and vGlut1 clusters (clusters/10 μm) along dendrites (shafts and/or protrusions) of DA-GFP were not different from those of GFP neurons (syn, 1.1±0.4 vs 1.2±0.4, *P*=0.7; vGlut1, 3.9±0.4 vs 3.9±0.4, *P*=0.87; *n*≥32 dendrites; Student's *t*-test) (Fig. 4J). However, in DA-GFP neurons, most protrusions (over 98%) were associated with clusters of synaptophysin or vGlut1, suggesting that the majority of protrusions had a presynaptic partner, similar to spines of GFP neurons. Since DA-GFP increased the dendritic spine density and the glutamatergic synaptic activity, we concluded that the density of glutamatergic synapses was increased in DA-GFP neurons.

The postsynaptic expression of DA-GFP did not affect the density of GABA presynaptic terminals in DA-GFP versus GFP neurons (Gad-65, 1.1±0.3 vs 1.2±0.5 clusters/10 μm; *n*≥32 dendrites; *P*=0.55; Student's *t*-test) (Fig. 4J). We next assessed whether the density of GABA synapses was affected in DA-GFP neurons. For this purpose we used β2,3 subunits of the $GABA_A$ receptor as a postsynaptic marker because β2,3 is one of the most abundant subunits of the $GABA_A$ receptors in the brain (McKernan and Whiting, 1996). Our data showed that the average density of clusters (clusters/10 μm) positive for β2,3 or for synaptophysin and β2,3 in DA-GFP was not different from that of GFP neurons (β2,3, 4.8±0.8 vs 4.5±0.8, *P*=0.51; β2,3 + syn, 1.4±0.5 vs 1.7±0.5, *P*=0.29; *n*≥32 dendrites; Student's *t*-test) (Fig. 4J). Therefore the densities of GABA terminals and synapses were similar in GFP and DA-GFP neurons. Taken together, these data indicated that the ratio of glutamatergic to GABAergic synapses was increased in DA-GFP neurons.

One possible explanation of the absence of significant changes in the density of presynaptic terminals in the presence of such marked changes in the density and shape of postsynaptic spines is that multiple spines can share the same terminal. If this is the case, multiple active zones should form, with a corresponding increase of active zone-associated proteins, such as bassoon. To assess this hypothesis, we studied the effects of DA overexpression on bassoon clusters (Fig. 5A,B‴). Our data showed that the average density of bassoon clusters (clusters/10 μm) along dendrites (shafts and/or protrusions) was increased in DA-GFP (28.2±1.9) compared with that of GFP neurons (16.8±2.0; *n*≥15 dendrites, *P*<0.0001; Student's

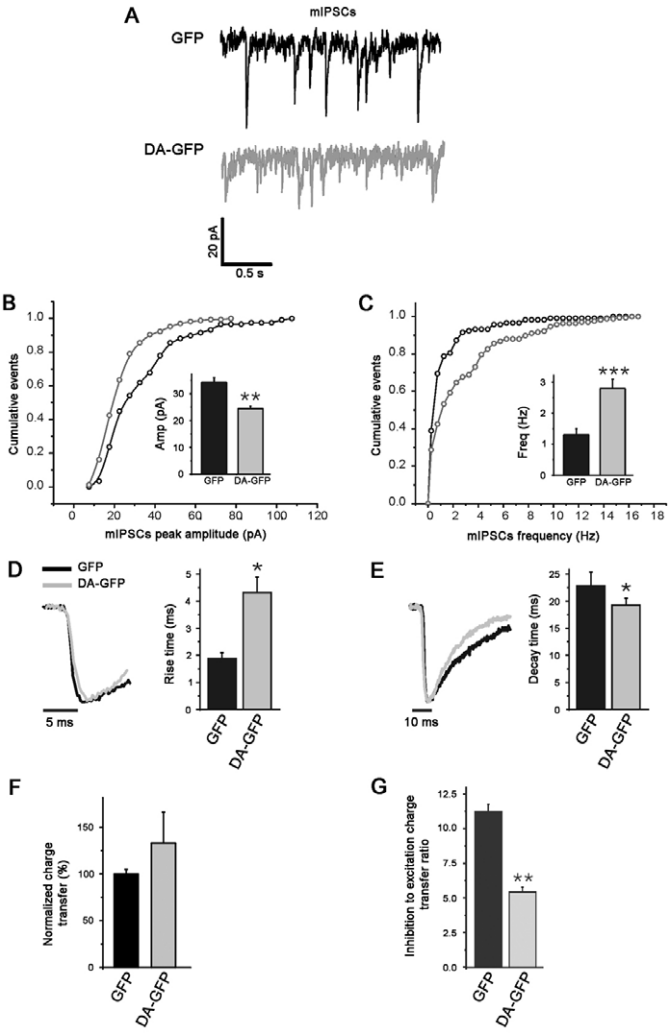

Fig. 3. Effects of DA-GFP overexpression on GABA function. Mixed hippocampal cultures were transfected at 21 DIV with GFP or DA-GFP, and 1 day later, the transfected neurons were recorded. Electrophysiological recordings of GFP neurons used as controls were compared with those of DA-GFP neurons. (A) Examples of mIPSCs recordings from GFP neurons (black trace) and DA-GFP neurons (gray trace). (B,C) Cumulative probability plots of amplitude and frequency of mIPSCs in GFP and DA-GFP neurons. The average amplitude (B) and frequency of mIPSCs (C) in GFP and DA-GFP neurons are shown in insets. ***P*<0.01, ****P*<0.001, K-S test. (D-G) Histograms showing the average rise time, decay time, charge transfer and inhibition to excitation transfer charge ratio of mEPSCs, respectively, in GFP and DA-GFP neurons. **P*<0.05, *t*-test; ***P*<0.01, U-test.

t-test) (Fig. 5C). Moreover, the average number of bassoon clusters on spines was increased almost twofold in DA-GFP neurons (1.9±0.2 vs 1.0±0.1 clusters/spine; $n \geqslant 15$ dendrites; $P<0.0001$; Student's *t*-test) (Fig. 5D). From these data, we concluded that indeed the increased number of spines was paralleled by an increase in the number of active zones.

Effects of downregulation of DA expression on synaptic function

Western blot analysis showed that treatment of mature mixed hippocampal cultures with DA antisense oligonucleotides (AS), whose specificity and efficiency have been described previously (Takahashi et al., 2003; Takahashi et al., 2006), reduced significantly the expression of endogenous DA (AS, 11.87±3.47%) when compared with untreated (Ctl, 100.00±14.77%; $n=7$; $P<0.0001$; Bonferroni's test) or sense-treated neurons (S, 84.59±12.91%; $n=7$; $P<0.001$; Bonferroni's test) (Fig. 6A,B, right panel). The expression of another neuronal protein such as β3-tubulin was not altered by oligonucleotide treatments when compared with untreated or sense-treated cultures (Ctl, 100.00±1.15%; S, 100.17±1.84%; AS, 100.21±1.68%; $n=7$; $P=0.99$; ANOVA) (Fig. 6A,B, left panel), in keeping with previously reported data for β-actin (Takahashi et al., 2003; Takahashi et al., 2006).

Whole-cell recordings of spontaneous and miniature synaptic currents were performed on mature cultured hippocampal neurons treated with sense oligonucleotides (used as a control, for details see supplementary material Fig. S4) or antisense oligonucleotides. Both sense and antisense oligonucleotide-treated neurons showed spontaneous activity (Fig. 6C), suggesting that these neurons were alive and fully integrated in the neuronal network. In addition, the neuronal network activity was not affected by the treatment with antisense oligonucleotides compared with that of neurons treated with sense oligonucleotides. Indeed, the average charge transfer of sPSCs was not significantly different in both culture types (S, 100±15%; AS, 92±21%; $n \geqslant 6$; $P=0.8$; U-test) (Fig. 6D).

The mEPSCs were recorded from S or AS neurons (Fig. 7A). In antisense-treated neurons, the cumulative probability plots of amplitude and frequency of mEPSCs were significantly shifted to lower values when compared to sense-treated neurons ($n=6$; $P<0.05$; K-S test) (Fig. 7B,C). The average amplitude and frequency of mEPSCs were decreased in antisense-treated neurons (11.3±0.9 pA; 4.3±1.5 Hz) when compared with those of sense-treated neurons (12.3±1.0 pA; 6.7±2.1 Hz) (Fig. 7B,C, insets). However, the average rise times (S, 1.44±0.16; AS, 1.58±0.15; $n=6$; $P=0.67$; Student's *t*-test) (Fig. 7D) and decay times (S, 4.42±0.65; AS, 4.67±0.61; $n=6$; $P=0.14$; Student's *t*-test) were comparable (Fig. 7E). As a result of amplitude and frequency changes of mEPSCs in antisense-treated neurons, the average charge transfer of mEPSCs was significantly reduced (56±3 vs 100±15%; $n=6$; $P<0.05$; U-test) (Fig. 7F).

We recorded the GABA mIPSCs from the same oligonucleotide-treated neurons, where the mEPSCs were recorded (Fig. 8A). In antisense-treated neurons, the cumulative probability plots of amplitude and frequency of mIPSCs were significantly shifted to lower values as compared with those of sense-treated neurons ($n=6$; $P<0.01$ for the amplitude and $P<0.05$ for the frequency; K-S test) (Fig. 8B,C). The average amplitude and frequency of mIPSCs were decreased in antisense-treated (15.9±1.6 pA; 2.3±0.7 Hz) when compared to sense-treated neurons (23.2±2.0 pA; 3.1±0.7 Hz) (Fig. 8B,C, insets). The average rise time and decay time of mIPSCs were not significantly modified in antisense-treated (3.52±0.44 mseconds; 20.48±1.78 mseconds) when compared with those of sense-treated neurons (2.74±0.31 mseconds; 22.25±3.30 mseconds; $n=6$; $P=0.12$ and 0.37 respectively; Student's *t*-test) (Fig. 8D,E). Owing to the mIPSC property changes described above, the average charge transfer in antisense-treated neurons was significantly reduced (78±11 vs 100±10%; $n=6$; $P<0.05$; U-test) (Fig. 8F). Thus, the reduction of DA expression affected both the functional properties of glutamatergic and GABAergic synapses. Despite these changes, the inhibition to excitation charge transfer ratio was not altered by the reduction of DA expression (AS, 7.7±2.8; S, 5.1±1.5; $n=6$; $P=0.9$; U-test) (Fig. 8G). Thus, the functional balance between excitation and inhibition was maintained while DA level was reduced.

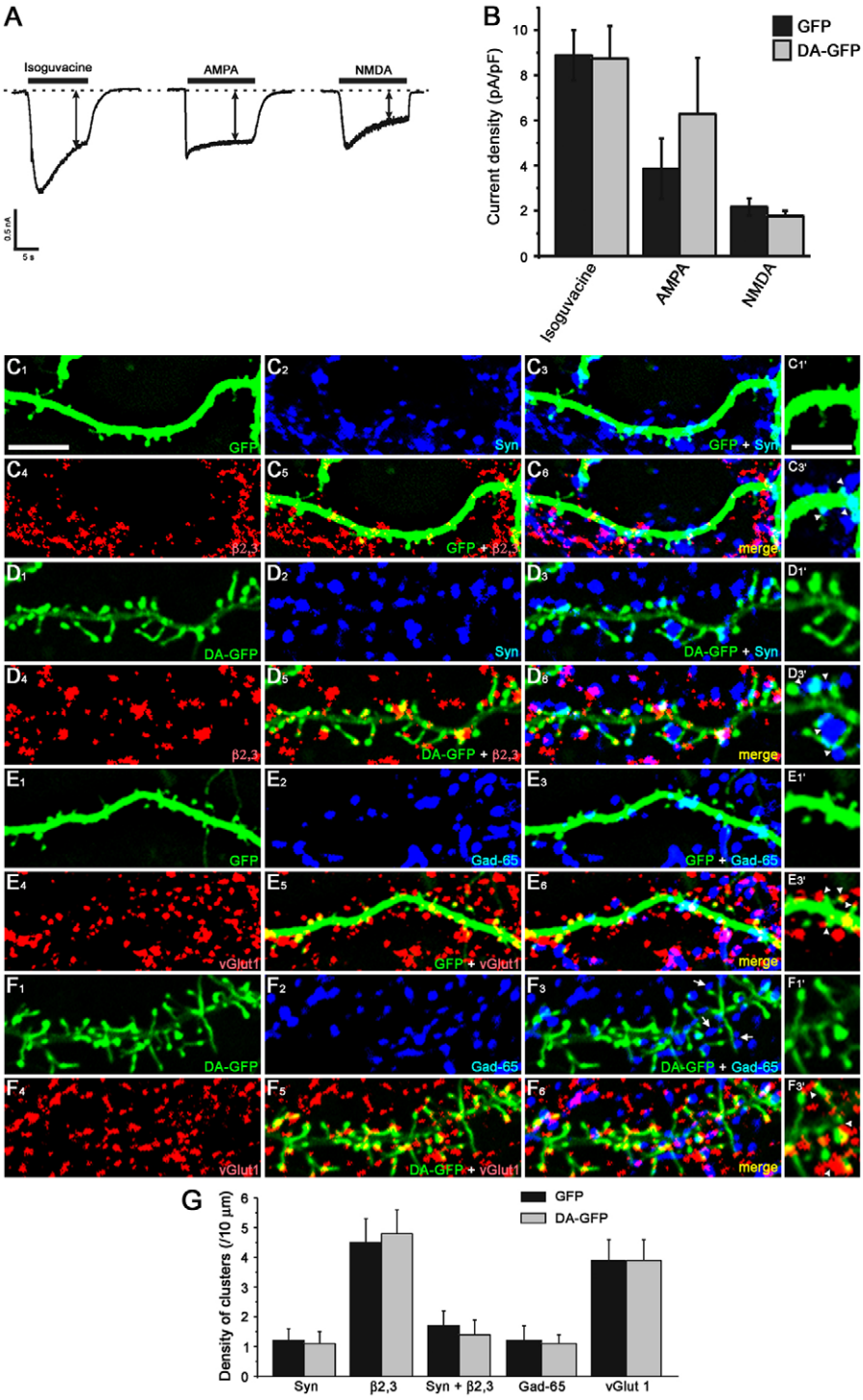

Fig. 4. Effects of DA-GFP on the density of GABA and glutamate receptors and synaptic proteins. Transfected neurons were recorded in whole-cell configuration at –60 mV for $GABA_A$- or AMPA-generated responses and –20 mV for NMDA-mediated current in the presence of TTX and strychnine. (A) Example of current responses induced by bath application of receptor agonists, Isoguvacine (20 µM), AMPA (100 µM) and NMDA (50 µM, with 10 µM glycine, NMDA coactivator) to activate $GABA_A$, AMPA and NMDA receptors, respectively, 10 seconds after starting perfusion (double arrows) with agonist-containing solution. (B) Quantitative analysis revealed that DA overexpression did not modify significantly the average current density of the agonist-mediated responses compared with that of GFP neurons. (C) Mixed hippocampal cultures were transfected at 21 DIV with GFP (C_1,E_1 and insets $C_{1'}$,$E_{1'}$) or DA-GFP (D_1,F_1 and insets $D_{1'}$,$F_{1'}$), and 1 day after transfection, cells were double immunostained for synaptophysin (C_2,D_2) and the subunit β2,3 of $GABA_A$ receptors (C_4,D_4) or for Gad-65 (E_2,F_2) and vGlut1 (E_4,F_4). All the synaptic markers were located either on the dendritic shafts or on dendritic protrusions. Interestingly, we observed in DA neurons that several dendritic spines share the same presynaptic terminal (see arrowheads in $D_{3'}$ vs $C_{3'}$ and $F_{3'}$ vs $E_{3'}$). Scale bars: 10 µm in C_1-F_6 and 5 µm in insets in right column. (G) The average density of syn, β2,3, syn + β2,3, Gad-65 and vGlut1 clusters along dendrites of DA-GFP were not different from those of GFP neurons. Note that in addition to dendrites of transfected neurons, all synaptic markers also stained dendrites of nontransfected neurons.

Discussion

This study provides the first evidence that DA can modulate both glutamatergic and GABAergic synaptic activities through regulation of spine plasticity.

Actin-binding domain of drebrin A is involved in spine plasticity

Our data clearly demonstrate that overexpression of DA increases spine density in mature hippocampal neurons. This finding is in keeping with the work of Takahashi and colleagues (Takahashi et al., 2003; Takahashi et al., 2006), who showed that downregulation of DA by antisense oligonucleotide treatment significantly decreased the density of filopodia spines. Altogether, these data strongly suggest that DA is involved in spine formation. The modification of the dynamic turnover of dendritic spines by stabilisation of F-actin might be one of the possible mechanisms leading to increased spine density. Indeed, we show that DA overexpression in CHO-K1 cells protects F-actin from cytochalasin B destabilization (supplementary material Fig. S3). Consistent with these findings, earlier studies also showed that DA expression in fibroblasts induced cytochalasin-D-resistant actin structures at their adhesion

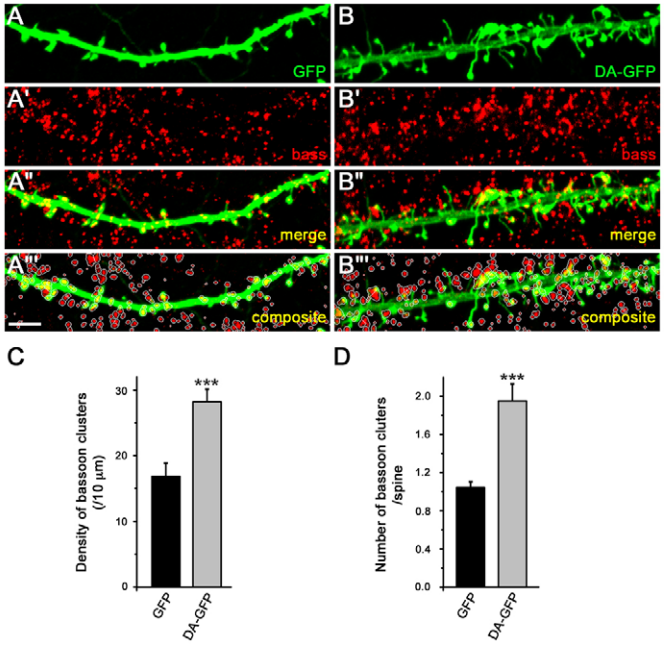

Fig. 5. Effects of DA-GFP overexpression on bassoon protein. Mixed hippocampal cultures were transfected at 21 DIV with GFP (A) or DA-GFP (B) and 1 day after transfection, cells were immunostained for bassoon (A′,B′). (A″ and B″) Merge of panels A and A′ and B and B′, respectively. (A‴ and B‴) Composite of A″ and B″, and drawings showing selected objects obtained with ImageJ software from A′ and B′, respectively. (C,D) Histograms showing the density of bassoon clusters (C) and their number per spine (D) in GFP and DA-GFP neurons. ***P<0.0001, Student's t-test. Scale bar: 5 µm.

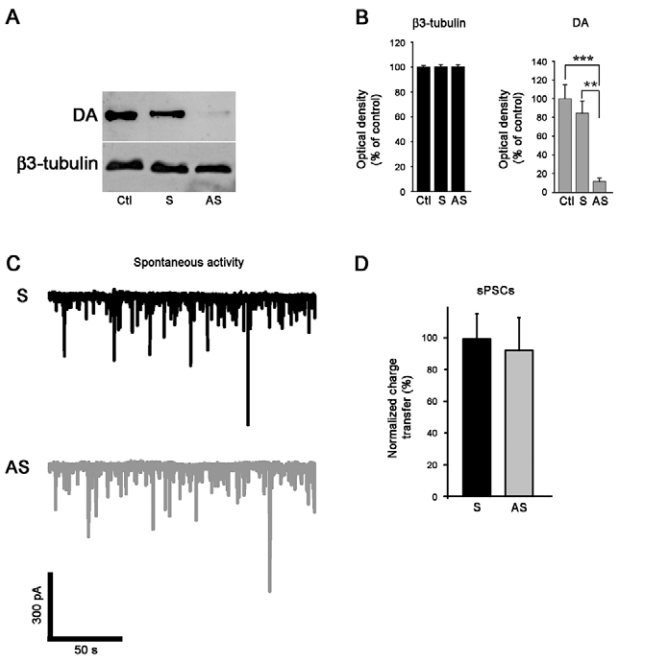

Fig. 6. Effects of DA downregulation on network activity. Mixed hippocampal cultures of 21 DIV treated for 2 days in the absence (untreated) or the presence of 10 µM sense (S) or antisense (AS) oligonucleotides. Following treatment, the cells were either used for western blot analysis (A,B) or electrophysiology recordings (C,D). **P<0.001, Bonferroni's test. (C) Using whole-cell recordings, sPSCs were detected at –60 mV in sense- (black trace) and antisense-treated neurons (gray trace). (D) Histogram showing the sPSC average charge transfer in all recorded neurons.

plaques (Ikeda et al., 1996). It is thus possible that elevated DA levels stabilize actin filaments in spines and alter their dynamic turnover (retraction). This inhibition of spine retraction by DA might lead to the increase in spine density.

In addition, our data show that DA regulates spine shape and size. Indeed, DA-GFP overexpression in mature cultured hippocampal neurons caused elongation of dendritic spines, which were similar to the spines observed in GFP-DA-expressing cortical neurons (Hayashi and Shirao, 1999). Furthermore, DA-GFP increases spine head width. This finding is corroborated by studies showing that downregulation of DA significantly decreases the width of filopodia spines (Takahashi et al., 2006). The morphological changes of dendritic spines induced by DA-GFP are mediated by its actin-binding domain as illustrated by our data (see Fig. 1A-G).

It has been reported that drebrin interacts directly with profilin (Mammoto et al., 1998), an actin-binding protein, known to stimulate actin polymerization (Carlsson et al., 1977; Buss et al., 1992; Rothkegel et al., 1996). One possible mechanism to induce morphological changes of dendritic spines is that DA recruits profilin to stimulate actin polymerization, leading to the elongation and increase in size of dendritic spines.

It has also been shown that DA reduced the movement of actin over a myosin-bound surface in the sliding actin motility assay, and inhibited the actin-based ATPase activity of myosin (Hayashi et al., 1996). The actomyosin-based machinery might thus be another mechanism involved in the elongation of spines. Based on these observations, we suggest that elongation of spines induced by DA-GFP may result from the superimposition of two additive mechanisms: polymerization of actin and inhibition of actomyosin activity and that DA is a key protein in the plasticity of dendritic spines.

DA modulates glutamatergic and GABAergic synaptic transmission

Our data showed that the long protrusions induced by DA are associated with presynaptic glutamatergic terminals. Despite the increased spine density (by about 43%), the density of glutamatergic terminals is not modified. However, the average number of active zone-associated bassoon clusters on spines is increased twice. Since bassoon is a component of the presynaptic apparatus of both excitatory glutamatergic and inhibitory GABAergic synapses (Richter et al., 1999), the increase of bassoon clusters suggests that at least some of the dendritic spines share the same glutamatergic terminal. Consistent with this idea, a single glutamatergic terminal could be contacted by two DA dendritic spines (see arrowheads in Fig. 4). As a result, the density of glutamatergic synapses is increased. Furthermore, our electrophysiological data demonstrate that these synapses are functional and more active. Indeed, an increase in the frequency (~27%) and amplitude (~18%) of mEPSCs were observed in DA-GFP neurons. The frequency increase could result from the augmented number of functional excitatory synapses, whereas the amplitude increase could be due to spine head widening (~13%) and/or to simultaneous glutamate release at multiple active sites. Bath application of glutamatergic agonists showed that overall density of receptors is preserved in DA-GFP neurons. This method does not permit us to distinguish the response mediated by extrasynaptic receptors from that mediated by synaptic receptors.

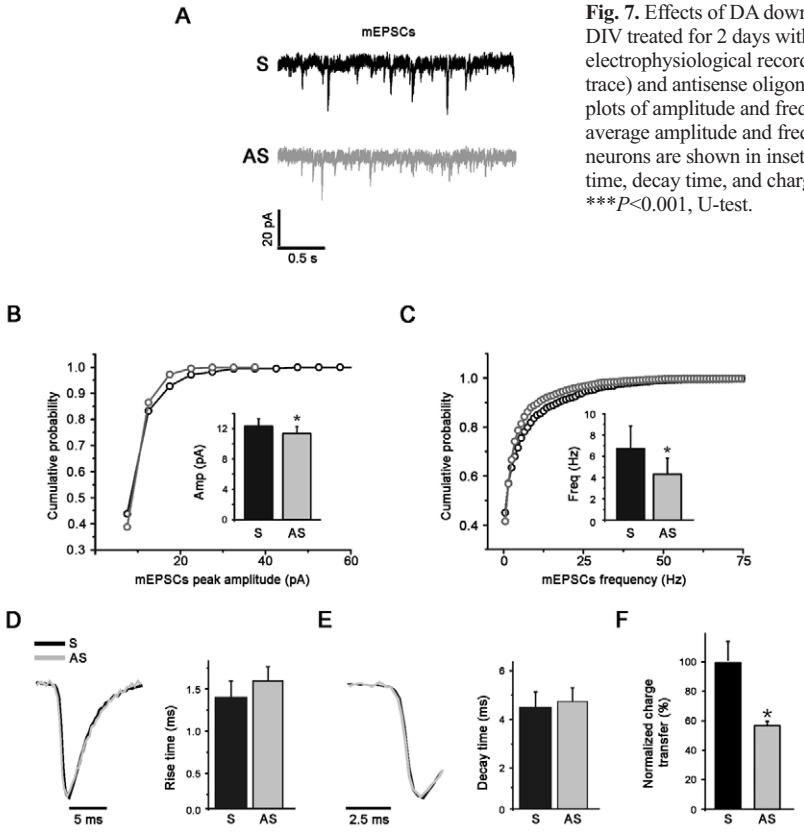

Fig. 7. Effects of DA downregulation on glutamate function. Mixed hippocampal cultures of 21 DIV treated for 2 days with 10 μM sense or antisense oligonucleotides, followed by electrophysiological recording. (A) Examples of mEPSCs recordings from DA sense (black trace) and antisense oligonucleotide-treated neurons (gray trace). (B,C) Cumulative probability plots of amplitude and frequency of mEPSCs in sense- and antisense-treated neurons. The average amplitude and frequency of mEPSCs in sense and antisense oligonucleotide-treated neurons are shown in insets. *P<0.05, K-S test. (D-F) Histograms showing the average rise time, decay time, and charge transfer of mEPSCs in oligonucleotide-treated neurons. ***P<0.001, U-test.

Therefore, these results show that overall density of glutamatergic membrane receptors (extrasynaptic and synaptic) was comparable in both GFP and DA-GFP neurons. Thus, the increased amplitude of mEPSCs could be explained by the spine head widening and the redistribution of glutamatergic extrasynaptic receptors to synaptic sites. The fact that the mEPSC kinetics was comparable in GFP and DA-GFP neurons, suggests that the subunit composition of glutamate receptors was not different in the newly formed and the already established excitatory synapses of DA neurons.

Despite a 43% increase in the density of excitatory synapses in DA-GFP neurons, we did not observe an equivalent increase in mEPSC frequency. This could suggest that synapses on dendritic shafts move on newly formed spines and/or that some of the DA-GFP excitatory synapses are inactive. In both cases, DA-GFP overexpression resulted in a significant increase in excitatory synaptic activity. As a result of the amplitude and frequency changes of mEPSCs in DA-GFP neurons, the glutamatergic transmission efficacy was significantly increased in DA-GFP compared with that of GFP neurons.

Our data revealed that although the mIPSC properties change (frequency, amplitude, and kinetics), the GABAergic transmission efficacy in DA-GFP neurons was not significantly different. The possible mechanisms that mediate the effect of DA on GABA postsynaptic activity are unknown. However it is interesting that DA could interact with gephyrin, a $GABA_A$ receptor anchoring protein (Kneussel and Loebrich, 2007), through profilin (Mammoto et al., 1998). Immunocytochemical data showed that the density of GABA synapses was also similar in GFP and DA-GFP neurons. As a result, the average inhibition to excitation charge transfer ratio is significantly reduced in DA-GFP neurons. Altogether, these observations indicate that DA-GFP overexpression increases the density of excitatory relative to inhibitory synapses, and enhances the excitation to inhibition ratio. The excitatory to inhibitory synapse ratio is believed to be crucial for normal neuronal computation and is generally kept constant by homeostatic mechanisms (Burrone et al., 2002; Hausser et al., 2000; Knott et al., 2002; Liu, 2004; Turrigiano and Nelson, 2004). Some of the factors that control the overall change in the ratio of excitatory-inhibitory synapse number and activity have only recently been discovered. Several studies have implicated the synaptic cell adhesion molecules called neuroligin (NLG) proteins and the scaffolding postsynaptic density protein PSD-95 (Prange et al., 2004; Chih et al., 2005; Levinson et al., 2005; Levinson and El Husseini, 2005a; Levinson and El Husseini, 2005b). An alteration in the excitation-inhibition synaptic balance was also suggested to occur in several neurodevelopmental psychiatric disorders, including autism and some forms of mental retardation (Rubenstein and Merzenich, 2003; Levinson and El Husseini, 2005a; Levinson and El Husseini, 2005b). The importance of our findings is emphasized by the recent discovery that the drebrin level is increased in the superior frontal cortex in neurological disorders accompanied by mild cognitive impairment (MCI) (Counts et al., 2006; Kojima and Shirao, 2007). It has been suggested that this might be a compensatory reaction to the reduced synaptic function in MCI.

Since overexpression of DA affected the glutamate and GABA synaptic properties, we investigated the functional consequences of a reduced DA expression. In DA-knockdown neurons, both amplitude and frequency of mEPSCs were reduced. The decreased amplitude of mEPSCs could be explained by the decreased in the width of filopodia spines observed in DA-knockdown neurons (Takahashi et al., 2006). The decreased frequency of mEPSCs in DA-knockdown neurons could be due to the decreased number of functional excitatory synapses. This possibility is supported by the fact that DA-knockdown neurons displayed a significant decrease in the density of filopodia spines (Takahashi et al., 2003; Takahashi et al., 2006). Similarly to mEPSCs, the frequency and amplitude of mIPSCs were also reduced in DA-knockdown neurons. These decreases could be due to the loss of dendritic spines containing functional inhibitory synapses (see arrows in Fig. 4F). Spines receiving both an excitatory and inhibitory input were first described by Jones and Powell (Jones and Powell, 1969) in the cat somatosensory cortex, and have since been implicated in inhibitory mechanisms by which the inhibitory synapses can reduce the excitatory influence of other synapses (Dehay et al., 1991; Knott et al., 2002). The fact that the kinetics of mEPSCs and mIPSCs were not affected by DA knockdown, suggests that the subunit composition of the glutamate and GABA receptor channels were not different in residual glutamatergic and GABAergic synapses, respectively, of DA-knockdown neurons. The parallel effects

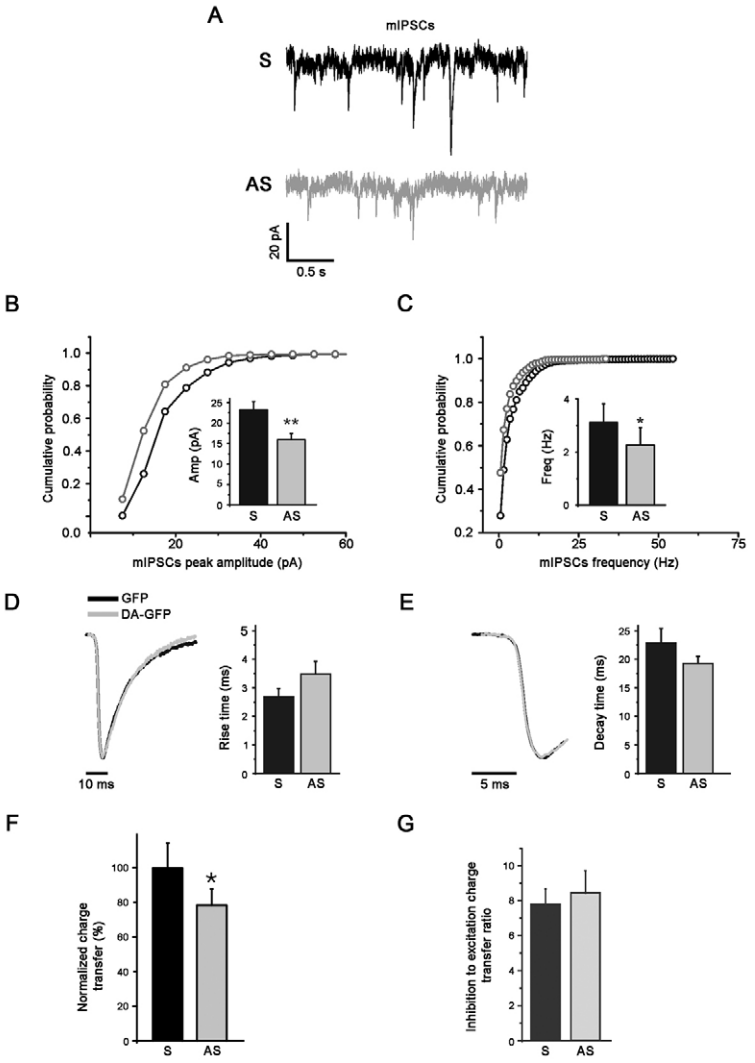

Fig. 8. Effects of DA downregulation on GABA function. Mixed hippocampal cultures of 21 DIV treated for 2 days with 10 µM sense (S) or antisense (AS) DA oligonucleotides, followed by electrophysiological recording. (A) Examples of mIPSC recordings from sense (black trace) and antisense neurons (gray trace). (B,C) Cumulative probability plots of amplitude and frequency of mIPSCs in sense and antisense oligonucleotide-treated neurons. The average amplitude and frequency of mIPSCs in oligonucleotide-treated neurons are shown in insets. **P*<0.05, ***P*<0.01, K-S test. (D-G) Histograms showing the average rise time, decay time, charge transfer and inhibition to excitation charge transfer ratio of mIPSCs in oligonucleotide-treated neurons. ****P*<0.001, U-test.

exerted by DA knockdown on mEPSCs and mIPSCs resulted in the reduction of both glutamatergic and GABAergic transmission efficacy. Despite these changes, the inhibition to excitation ratio was not affected by the 73% reduction of DA expression. Combined with the data described above, these results indicated that the residual DA was not sufficient to affect the functional balance between excitation and inhibition. One possible explanation of the effects of DA on the inhibitory to excitatory ratio is that in the case of overexpression of DA we affect only transfected postsynaptic neurons, whereas in the case of underexpression of DA we also affect the presynaptic neurons. Thus, the amounts of DA available can contribute to the homeostatic mechanism that maintains the structural and functional balance between excitatory and inhibitory synapses.

Interestingly, a decreased level in DA content is reported in the superior temporal cortex in MCI and Alzheimer disease (Counts et al., 2006; Kojima and Shirao, 2007). In addition, the level of postsynaptic DA has been shown to strongly correlate with the severity of cognitive impairment (Counts et al., 2006; Kojima and Shirao, 2007). This indicated that a critical level of DA protein might be required for normal function. Therefore, we propose a model in which improper expression of DA might trigger either an imbalance in neuronal excitability or an alteration in synaptic transmission. In both cases, these alterations result in synaptic dysfunction reminiscent of that observed in the cognitive impairment accompanying normal aging and neurological disorders, including Alzheimer disease (Harigaya et al., 1996; Hatanpää et al., 1999; Counts et al., 2006; Kojima and Shirao, 2007) and Down syndrome (Shim and Lubec, 2002).

In conclusion, the identification of factors involved in synaptogenesis should enhance our understanding of the mechanisms responsible for synaptic plasticity as well as the cellular and molecular defects observed in neurological disorders.

Materials and Methods

cDNA constructs

The full-length drebrin A (DA, NCBI accession number NM-031024) fragment was amplified by PCR and inserted into pEGFP-N1 vector (BD Bioscience Clontech, Palo Alto, CA). The DA-GFP construct was subsequently fully sequenced. We also used GFP-ABS and GFP-DAΔABS constructs (see Hayashi et al., 1999).

Cell lines, transfection and immunofluorescence

Chinese Ovary (CHO-K1) cells were obtained from the American Type Tissue Culture Collection (ATCC, Molsheim, France). They were grown in F12 (Invitrogen, Cergy Pontoise, France), supplemented with 10% fetal bovine serum (FBS, Invitrogen), 2 mM glutamine (Invitrogen), 100 U/ml penicillin and 100 mg/ml streptomycin (Sigma, Lyon, France). Cells were rinsed one time with serum-free medium (Opti-MEM, Invitrogen) and transfections were performed according to the manufacturer's protocol (Invitrogen). Briefly, cells were incubated in a solution containing 500 µl Opti-MEM, 4 µl Plus reagent, 6 µl lipofectamine reagent (Invitrogen) and 1 µg of either the GFP, the DA-GFP, the GFP-ABS or the GFP-DAΔABS construct. After incubation for 4 hours at 37°C, the transfection mixture was replaced by a fresh complete growth medium containing 10% FBS. 24 hours after transfection, cells were fixed with 4% paraformaldehyde (PFA) in 0.12 M phosphate buffer (PB), pH 7.2-7.4 for 20 minutes at room temperature (RT).

Quantitative analyses of the number of transfected cells were performed using a fluorescence microscope with a ×20 objective. Twenty fields per coverslip per experiment (n=3) were analyzed. Data were expressed as mean % of total cells per experiment ± s.e.m.

For the F-actin staining, the cells were incubated with 0.5% Triton X-100 and 1% blocking reagent (BR, Roche, Meylan, France) for 30 minutes and exposed for 2 hours at RT to 0.5 U per coverslip of Texas-Red-labeled X phalloidin (Molecular Probes, Leiden, Netherlands), rinsed in PB and incubated with 0.5 µg/ml DNA intercalant Hoechst 33258 (Molecular Probes). Cells were rinsed in PB and then mounted with Fluoromount G (Electron Microscopy, Fort Washington, PA).

In some experimental sets (n=3), the microfilament-depolymerizing drug cytochalasin B (Sigma, used at 10 µg/ml final concentration in 0.1% dimethylsulfoxide) was added into the medium to assess the stability of F-actin of transfected cells. After incubation with cytochalasin B for 10 minutes, cells were fixed with PFA for 20 minutes, washed three times with PB, stained for F-actin as described above, rinsed in PB, then incubated with Hoechst 33258, and mounted with Fluoromount G.

Analysis was performed on a Leica (Mannheim, Germany) TCS SP2 confocal microscope using the 488 nm band of an Ar laser and the 543 nm band of a He-Ne laser for excitation of GFP and Texas Red, respectively. Images were acquired by sequential scanning using ×63 1.32 oil-immersion lens (zoom 3) and processed with Adobe Photoshop. Results are shown in supplementary material Figs S1-S4.

Primary cultures of rat hippocampal neurons and transfection

Mixed hippocampal cultures were prepared from embryonic day 18 (E18) rats according to Rami et al. (Rami et al., 2006). At 21 DIV, mixed hippocampal cultures were transiently transfected using a Magnetofection Kit (OZ Biosciences, Marseille, France) and lipofectamine 2000 reagent according to the OZ Biosciences protocol. Following transfection, the cells were either used for electrophysiology recordings or fixed with 4% PFA in 0.12 M phosphate buffer (PB), pH 7.2-7.4 for 20 minutes at RT for immunofluorescence. The transfection efficiency was less than 1%.

Immunofluorescence

For single immunolabeling of DA and double immunolabeling of DA/synaptophysin and DA/PSD-95, mixed hippocampal cultures of 21 DIV were incubated overnight at RT in DA antiserum (1:500) (Aoki et al., 2005) or a mixture of DA antiserum and either synaptophysin (1:300, Chemicon, Temecula, CA), or PSD-95 (1:500, Upstate, Charlottesville, VA) monoclonal antibodies diluted in PB containing 1% BR. After several rinses in PB, coverslips were incubated in a mixture of Alexa 488-conjugated goat anti-rabbit IgG and Cy3-conjugated goat anti-mouse IgG (1:200, both from Jackson Immunoresearch, West Grove, PA) diluted in PB containing 1% BR.

For double labeling of DA/F-actin, cells were exposed for 2 hours at RT to 0.5 U per coverslip of Texas-Red X phalloidin prepared in PB containing 1% BR.

Single immunolabeling of bassoon, double immunolabeling of synaptophysin/β2,3 or Gad-65/vGlut1 were performed on hippocampal neurons transfected with GFP or DA-GFP. Cells were incubated with the following primary antibodies (most from Chemicon): polyclonal synaptophysin (1:500) and mouse monoclonal antibody against $GABA_A$ receptor beta chain (β2,3, 1:500) or mouse monoclonal antibody against Gad 65 (one of the glutamic acid decarboxylase isoforms, 1:300) and guinea pig polyclonal antiserum against vGlut1 (vesicular glutamate transporter 1, 1:5000) or mouse monoclonal antibody against bassoon (1:300, Assay designs, Ann Arbor, MI). After several rinses in PB, coverslips were incubated for 1 hour at RT in biotinylated goat- anti-rabbit IgG (1:200) or anti-mouse IgG (1:200), and then incubated in a mixture of Cy5-conjugated streptavidin and Cy3-conjugated goat anti-mouse IgG or Cy3-conjugated donkey anti-guinea pig IgG (1:200, all from Jackson Immunoresearch). Bassoon staining was revealed with Alexa Fluor 594-conjugated goat anti-mouse IgG (1:200, Molecular Probes) diluted in PB containing 1% BR. In all cases, no labeling was detected when specific antibodies were replaced with normal rabbit, mouse, guinea pig serum or when primary antibodies were omitted.

Image acquisition and quantification

All measurements were performed on spiny and pyramidal neurons that were visually identified based on their morphology (Benson et al., 1994). Images were acquired with an Olympus fluoview-500 confocal microscope (Olympus, France) using an oil immersion ×60 1.4 lens (zoom 3). Dendritic protrusions were reconstructed from 7 to 15 serial images of 0.5 μm thickness projected onto one plane. For morphometric analysis, protrusion length, width and density were measured from projected images using Neurolucida software as described previously (Rami et al., 2006).

Analysis of synaptic proteins was performed with an Olympus Fluoview-500 confocal microscope using the 488, 543, 633 laser lines for excitation of GFP, Cy3 and Cy5, respectively. For quantitation of synaptic protein clusters, pictures from GFP and DA-GFP neurons were taken sequentially using ×63 1.4 (zoom 3) with the same exposure parameters. Then the projections of z-stacks were thresholded equally to eliminate the background of dendritic staining and the remaining clusters were counted based on their location either on dendritic shafts or on dendritic protrusions using Neurolucida or ImageJ softwares. Five to ten transfected neurons were chosen randomly from three independent experiments for GFP and DA-GFP constructs and the number of clusters was collected from at least three dendritic segments of 100 μm per neuron. Then, the density of the synaptic protein clusters was determined similarly to protrusion density.

Westerns blot analysis

For western blot analysis, cultures were homogenized in 50 mM Tris-HCl, pH 6.8, 5% SDS, 6% 2-mercaptoethanol, 10% glycerol and 4 mM EDTA. Protein samples were boiled for 10 minutes, and equal amounts were loaded into each well, resolved on 8% SDS-polyacrylamide gels and transferred onto Hybond-ECL nitrocellulose membranes (Amersham Biosciences, Germany). Blots were then blocked, immunostained with appropriate antibodies and immunodetected using the enhance chemiluminescence system (ECL, Amersham Biosciences). Chemiluminescent signals were projected on X-ray film and digitalized, and the signals were quantified using ImageJ.

Antisense experiments

Translation of DA was suppressed by treatment of cultures with an antisense phosphorothioate-substituted DNA oligonucleotides (AS) (Takahashi et al., 2006). The sense phosphorothioate oligonucleotide (S) (Takahashi et al., 2006) was used as negative control since the sense oligo treatment has no effect on the expression of DA, β3-tubulin and synaptic activity compared with untreated cultures (supplementary material Fig. S4). Therefore, we used sense oligo-treated neurons for the analysis of the control neuronal activity. At 21 DIV, cultures were treated for 2 days in the absence (untreated) or the presence of 10 μM sense or antisense oligonucleotides. Following treatment, the cells were either used for western blot analysis or electrophysiology recordings.

Whole-cell recording

sPSCs or mPSCs were recorded from visually identified spiny and pyramidal neurons (Chudotvorova et al., 2005; Rami et al., 2006). The mEPSCs or mIPSCs were isolated at –60 mV in the presence of TTX, D-AP5, strychnine and bicuculline/CNQX. We took into account for analysis, only neurons in which both mEPSCs and mIPSCs were recorded. To evaluate the change produced by DA-GFP overexpression or by treatment with antisense oligonucleotides against DA on network activity and the overall synaptic strength of a single neuron (Turrigiano et al., 1998; Burrone et al., 2002; Liu, 2004; Chih et al., 2005), the mean charge transfer was determined. This parameter depends simultaneously on the amplitude, frequency and kinetic of postsynaptic currents. Therefore, during spontaneous activity, charge transfer reflects neuronal network activity. When this activity is blocked by TTX, the charge transfer reflects the overall synaptic strength of a single neuron (Liu, 2004). Charge transfers for sPSCs or mPSCs were calculated for each recorded neuron as the sPSCs or mPSCs area (charge transferred by single postsynaptic current) multiplied on instantaneous frequency value (instantaneous frequency=1/inter-event interval). In each experiment, the mean charge transfer values were normalized relative to the average mean control value (expressed in %). To evaluate the effects of postsynaptic receptor agonists within different cells, the current densities (amplitude/cell capacitance) were compared. Amplitudes of currents induced by bath application of agonists were measured 10 seconds after starting perfusion with agonist containing solution (see Fig. 4A).

Statistical analysis

All experiments were repeated at least three times with different culture series. Morphological, immunostaining and western blot data were statistically analyzed by unpaired Student's *t*-test for comparing two groups, or by ANOVA, with *a* post hoc Bonferroni's *t*-test (Bonferroni test) for multiple comparison, as applicable.

Statistical analyses for frequency, amplitude, and area of mPSCs were performed with the nonparametric Kolmogorov-Smirnov (K-S) test. Unpaired Student's *t*-test was used to examine the statistical significance of the differences between groups of others parameters (decay time, rise time, density of agonist induced current). All data parameters were expressed as the mean ± s.e.m. To determine the difference between groups of charge transfer data, Kolmogorov-Smirnov as well as Mann-Whitney U (U-test) tests were used; the higher value of *P* was taken into account.

We thank Djaffar Boussa, Santiago Rivera, François Feron and Michel Khrestchatisky for critical reading of the manuscript. We also thank Marie-Pierre Blanchard for her help with the Leica laser microscope. This work was supported by grants from the Institut National de la Santé et de la Recherche Médicale (INSERM) and the Centre National de la Recherche Scientifique (CNRS). This project was initiated in the INMED laboratory directed by Yezekiel Ben Ari.

References

Aoki, C., Sekino, Y., Hanamura, K., Fujisawa, S., Mahadomrongkul, V., Ren, Y. and Shirao, T. (2005). Drebrin A is a postsynaptic protein that localizes in vivo to the submembranous surface of dendritic sites forming excitatory synapses. *J. Comp. Neurol.* **483**, 383-402.

Ballestrem, C., Wehrle-Haller, B. and Imhof, B. A. (1998). Actin dynamics in living mammalian cells. *J. Cell Sci.* **111**, 1649-1658.

Benson, D. L., Watkins, F. H., Steward, O. and Banker, G. (1994). Characterization of GABAergic neurons in hippocampal cell cultures. *J. Neurocytol.* **23**, 279-295.

Burrone, J., O'Byrne, M. and Murthy, V. N. (2002). Multiple forms of synaptic plasticity triggered by selective suppression of activity in individual neurons. *Nature* **420**, 414-418.

Buss, F., Temm-Grove, C., Henning, S. and Jockusch, B. M. (1992). Distribution of profilin in fibroblasts correlates with the presence of highly dynamic actin filaments. *Cell Motil. Cytoskeleton* **22**, 51-61.

Carlsson, L., Nystrom, L. E., Sundkvist, I., Markey, F. and Lindberg, U. (1977). Actin polymerizability is influenced by profilin, a low molecular weight protein in non-muscle cells. *J. Mol. Biol.* **115**, 465-483.

Chih, B., Engelman, H. and Scheiffele, P. (2005). Control of excitatory and inhibitory synapse formation by neuroligins. *Science* **307**, 1324-1328.

Chudotvorova, I., Ivanov, A., Rama, S., Hübner, C. A., Pellegrino, C., Ben-Ari, Y. and Medina, I. (2005). Early expression of KCC2 in rat hippocampal cultures augments expression of functional GABA synapses. *J. Physiol.* **566**, 671-679.

Cooper, J. A. (1987). Effects of cytochalasin and phalloidin on actin. *J. Cell Biol.* **105**, 1473-1478.

Counts, S. E., Nadeem, M., Lad, S. P., Wuu, J. and Mufson, E. J. (2006). Differential expression of synaptic proteins in the frontal and temporal cortex of elderly subjects with mild cognitive impairment. *J. Neuropathol. Exp. Neurol.* **65**, 592-601.

Dehay, C., Douglas, R. J., Martin, K. A. and Nelson, C. (1991). Excitation by geniculocortical synapses is not 'vetoed' at the level of dendritic spines in cat visual cortex. *J. Physiol.* **440**, 723-734.

Edson, K., Weisshaar, B. and Matus, A. (1993). Actin depolymerisation induces process formation on MAP2-transfected non-neuronal cells. *Development* **117**, 689-700.
Fifkova, E. and Delay, R. J. (1982). Cytoplasmic actin in neuronal processes as a possible mediator of synaptic plasticity. *J. Cell Biol.* **95**, 345-350.
Fukazawa, Y., Saitoh, Y., Ozawa, F., Ohta, Y., Mizuno, K. and Inokuchi, K. (2003). Hippocampal LTP is accompanied by enhanced F-actin content within the dendritic spine that is essential for late LTP maintenance *in vivo*. *Neuron* **38**, 447-460.
Harigaya, Y., Shoji, M., Shirao, T. and Hirai, S. (1996). Disappearance of actin-binding protein, drebrin, from hippocampal synapses in Alzheimer's disease. *J. Neurosci. Res.* **43**, 87-92.
Harris, K. M. and Kater, S. B. (1994). Dendritic spines: cellular specializations imparting both stability and flexibility to synaptic function. *Annu. Rev. Neurosci.* **17**, 341-371.
Hatanpaa, K., Isaacs, K. R., Shirao, T., Brady, D. R. and Rapoport, S. I. (1999). Loss of proteins regulating synaptic plasticity in normal aging of the human brain and in Alzheimer disease. *J. Neuropathol. Exp. Neurol.* **58**, 637-643.
Hausser, M., Spruston, N. and Stuart, G. J. (2000). Diversity and dynamics of dendritic signaling. *Science* **290**, 739-744.
Hayashi, K. and Shirao, T. (1999). Change in the shape of dendritic spines caused by overexpression of drebrin in cultured cortical neurons. *J. Neurosci.* **19**, 3918-3925.
Hayashi, K., Ishikawa, R., Ye, L. H., He, X. L., Takata, K., Kohama, K. and Shirao, T. (1996). Modulatory role of drebrin on the cytoskeleton within dendritic spines in the rat cerebral cortex. *J. Neurosci.* **16**, 7161-7170.
Hayashi, K., Ishikawa, R., Kawai-Hirai, R., Takagi, T., Taketomi, A. and Shirao, T. (1999). Domain analysis of the actin-binding and actin-remodeling activities of drebrin. *Exp. Cell Res.* **253**, 673-680.
Ikeda, K., Kaub, P. A., Asada, H., Uyemura, K., Toya, S. and Shirao, T. (1996). Stabilization of adhesion plaques by the expression of drebrin A in fibroblasts. *Brain Res. Dev. Brain Res.* **91**, 227-236.
Ishikawa, R., Hayashi, K., Shirao, T., Xue, Y., Takagi, T., Sasaki, Y. and Kohama, K. (1994). Drebrin, a development-associated brain protein from rat embryo, causes the dissociation of tropomyosin from actin filaments. *J. Biol. Chem.* **269**, 29928-29933.
Ishikawa, R., Katoh, K., Takahashi, A., Xie, C., Oseki, K., Watanabe, M., Igarashi, M., Nakamura, A. and Kohama, K. (2007). Drebrin attenuates the interaction between actin and myosin-V. *Biochem. Biophys. Res. Commun.* **359**, 398-401.
Jones, E. G. and Powell, T. P. (1969). Morphological variations in the dendritic spines of the neocortex. *J. Cell Sci.* **5**, 509-529.
Kneussel, M. and Loebrich, S. (2007). Trafficking and synaptic anchoring of ionotropic inhibitory neurotransmitter receptors. *Biol. Cell* **99**, 297-309.
Knott, G. W., Quairiaux, C., Genoud, C. and Welker, E. (2002). Formation of dendritic spines with GABAergic synapses induced by whisker stimulation in adult mice. *Neuron* **34**, 265-273.
Kojima, N. and Shirao, T. (2007). Synaptic dysfunction and disruption of postsynaptic drebrin-actin complex: a study of neurological disorders accompanied by cognitive deficits. *Neurosci. Res.* **58**, 1-5.
Levinson, J. N. and El-Husseini, A. (2005a). Building excitatory and inhibitory synapses: balancing neuroligin partnerships. *Neuron* **48**, 171-174.
Levinson, J. N. and El-Husseini, A. (2005b). New players tip the scales in the balance between excitatory and inhibitory synapses. *Mol. Pain* **1**, 12.
Levinson, J. N., Chery, N., Huang, K., Wong, T. P., Gerrow, K., Kang, R., Prange, O., Wang, Y. T. and El-Husseini, A. (2005). Neuroligins mediate excitatory and inhibitory synapse formation: involvement of PSD-95 and neurexin-1beta in neuroligin-induced synaptic specificity. *J. Biol. Chem.* **280**, 17312-17319.
Liu, G. (2004). Local structural balance and functional interaction of excitatory and inhibitory synapses in hippocampal dendrites. *Nat. Neurosci.* **7**, 373-379.
Mammoto, A., Sasaki, T., Asakura, T., Hotta, I., Imamura, H., Takahashi, K., Matsuura, Y., Shirao, T. and Takai, Y. (1998). Interactions of drebrin and gephyrin with profilin. *Biochem. Biophys. Res. Commun.* **243**, 86-89.
Matus, A. (2000). Actin-based plasticity in dendritic spines. *Science* **290**, 754-758.
Matus, A., Ackermann, M., Pehling, G., Byers, H. R. and Fujiwara, K. (1982). High actin concentrations in brain dendritic spines and postsynaptic densities. *Proc. Natl. Acad. Sci. USA* **79**, 7590-7594.
McKernan, R. M. and Whiting, P. J. (1996). Which GABAA-receptor subtypes really occur in the brain? *Trends Neurosci.* **19**, 139-143.
Papa, M., Bundman, M. C., Greenberger, V. and Segal, M. (1995). Morphological analysis of dendritic spine development in primary cultures of hippocampal neurons. *J. Neurosci.* **15**, 1-11.
Prange, O., Wong, T. P., Gerrow, K., Wang, Y. T. and El-Husseini, A. (2004). A balance between excitatory and inhibitory synapses is controlled by PSD-95 and neuroligin. *Proc. Natl. Acad. Sci. USA* **101**, 13915-13920.
Rami, G., Caillard, O., Medina, I., Pellegrino, C., Fattoum, A., Ben-Ari, Y. and Ferhat, L. (2006). Change in the shape and density of dendritic spines caused by overexpression of acidic calponin in cultured hippocampal neurons. *Hippocampus* **16**, 183-197.
Richter, K., Langnaese, K., Kreutz, M. R., Olias, G., Zhai, R., Scheich, H., Garner, C. C. and Gundelfinger, E. D. (1999). Presynaptic cytomatrix protein bassoon is localized at both excitatory and inhibitory synapses of rat brain. *J. Comp. Neurol.* **408**, 437-448.
Rothkegel, M., Mayboroda, O., Rohde, M., Wucherpfennig, C., Valenta, R. and Jockusch, B. M. (1996). Plant and animal profilins are functionally equivalent and stabilize microfilaments in living animal cells. *J. Cell Sci.* **109**, 83-90.
Rubenstein, J. L. and Merzenich, M. M. (2003). Model of autism: increased ratio of excitation/inhibition in key neural systems. *Genes Brain Behav.* **2**, 255-267.
Sasaki, Y., Hayashi, K., Shirao, T., Ishikawa, R. and Kohama, K. (1996). Inhibition by drebrin of the actin-bundling activity of brain fascin, a protein localized in filopodia of growth cones. *J. Neurochem.* **66**, 980-988.
Sekino, Y., Kojima, N. and Shirao, T. (2007). Role of actin cytoskeleton in dendritic spine morphogenesis. *Neurochem. Int.* **51**, 92-104.
Shim, K. S. and Lubec, G. (2002). Drebrin, a dendritic spine protein, is manifold decreased in brains of patients with Alzheimer's disease and Down syndrome. *Neurosci. Lett.* **324**, 209-212.
Shirao, T., Hayashi, K., Ishikawa, R., Isa, K., Asada, H., Ikeda, K. and Uyemura, K. (1994). Formation of thick, curving bundles of actin by drebrin A expressed in fibroblasts. *Exp. Cell Res.* **215**, 145-153.
Takahashi, H., Sekino, Y., Tanaka, S., Mizui, T., Kishi, S. and Shirao, T. (2003). Drebrin-dependent actin clustering in dendritic filopodia governs synaptic targeting of postsynaptic density-95 and dendritic spine morphogenesis. *J. Neurosci.* **23**, 6586-6595.
Takahashi, H., Mizui, T. and Shirao, T. (2006). Down-regulation of drebrin A expression suppresses synaptic targeting of NMDA receptors in developing hippocampal neurones. *J. Neurochem.* **97 Suppl. 1**, 110-115.
Turrigiano, G. G. and Nelson, S. B. (2004). Homeostatic plasticity in the developing nervous system. *Nat. Rev Neurosci* **5**, 97-107.
Turrigiano, G. G., Leslie, K. R., Desai, N. S., Rutherford, L. C. and Nelson, S. B. (1998). Activity-dependent scaling of quantal amplitude in neocortical neurons. *Nature* **391**, 892-896.
Yahara, I., Harada, F., Sekita, S., Yoshihira, K. and Natori, S. (1982). Correlation between effects of 24 different cytochalasins on cellular structures and cellular events and those on actin *in vitro*. *J. Cell Biol.* **92**, 69-78.
Yuste, R. and Bonhoeffer, T. (2001). Morphological changes in dendritic spines associated with long-term synaptic plasticity. *Annu. Rev. Neurosci.* **24**, 1071-1089.